Supporting Information

for

Photothermal initiation of frontal polymerization using carbon nanoparticles

Leon M. Dean,[†,⊥] Amogha Ravindra,[†,⊥] Allen X. Guo,[†,⊥] Mostafa Yourdkhani,[§] and Nancy R. Sottos*[,†,⊥]

[†]Department of Materials Science and Engineering, [‡]Department of Aerospace Engineering, [⊥]Beckman Institute for Advanced Science and Technology, University of Illinois at Urbana-Champaign, Urbana, Illinois 61801, United States

[§]Department of Mechanical Engineering, Colorado State University, Fort Collins, Colorado 80523, United States

* Corresponding author. E-mail: n-sottos@illinois.edu

Table of Contents:

1. Optical Characterization of Nanoparticle Suspensions.

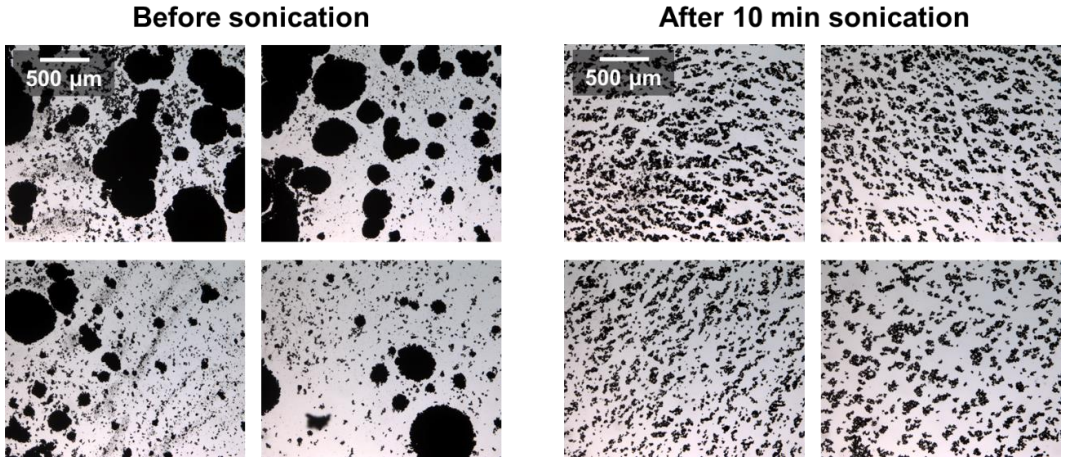

Figure S1. Representative optical micrographs of 1 wt% CB in DCPD suspensions showing the breakup of CB agglomerates during bath sonication. Further breakup was not observed for longer sonication times or through the use of horn sonication. Each sample is 6 µL of suspension sandwiched between a glass slide and a cover slip. The scale is the same for all images.

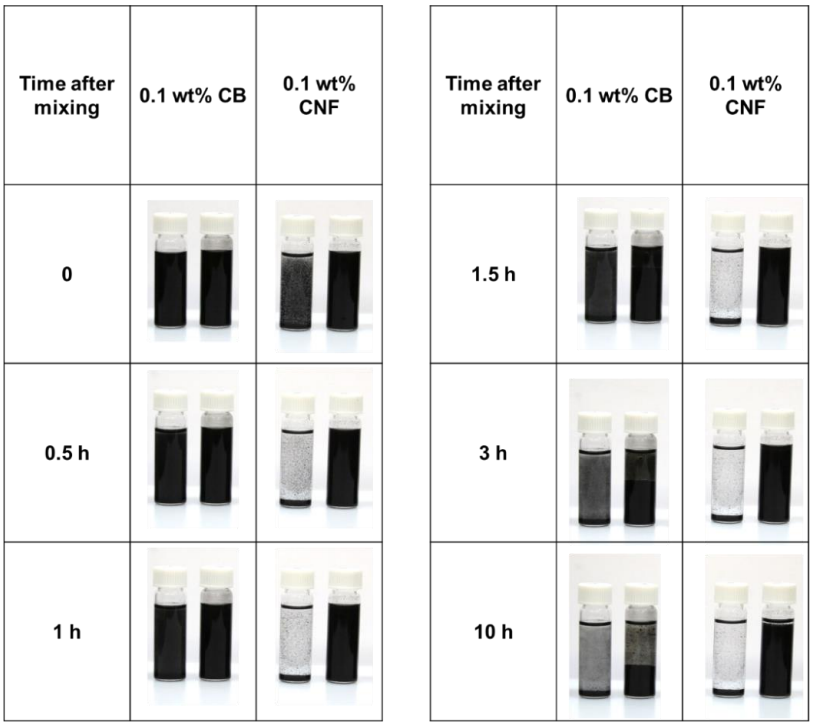

Figure S2. Optical images showing stability of nanoparticle suspensions in 8 mL vials. In each image, the suspension in the left vial was not sonicated and the suspension in the right vial was sonicated for 10 minutes. For the sonicated CB/DCPD suspension, noticeable sedimentation does not occur for 1.5 h. For the sonicated CNF/DCPD suspension, noticeable sedimentation does not occur for 3h.

2. UV-Vis Spectroscopy. CB/DCPD suspensions were loaded immediately after sonication into disposable cuvettes. UV-Vis absorption spectra were recorded on a Shimadzu UV-2401PC spectrometer. The spectra are shown in Figure S3.

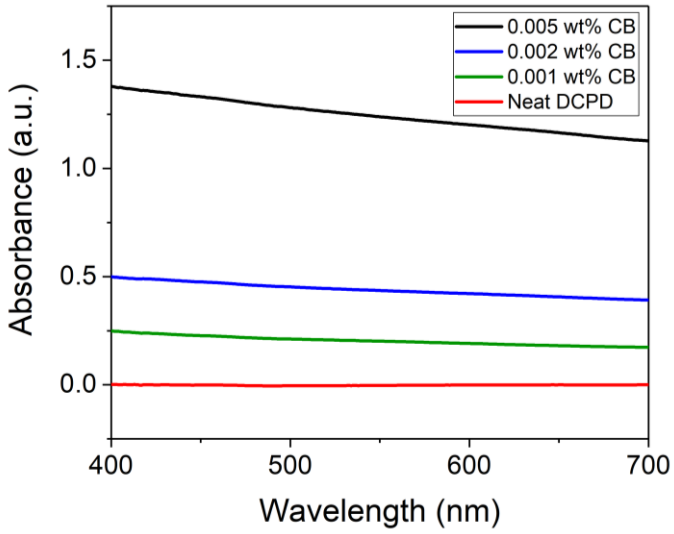

Figure S3. UV-Vis absorption spectra collected for suspensions with various loadings of CB in DCPD.

3. Light Source Emission Spectrum.

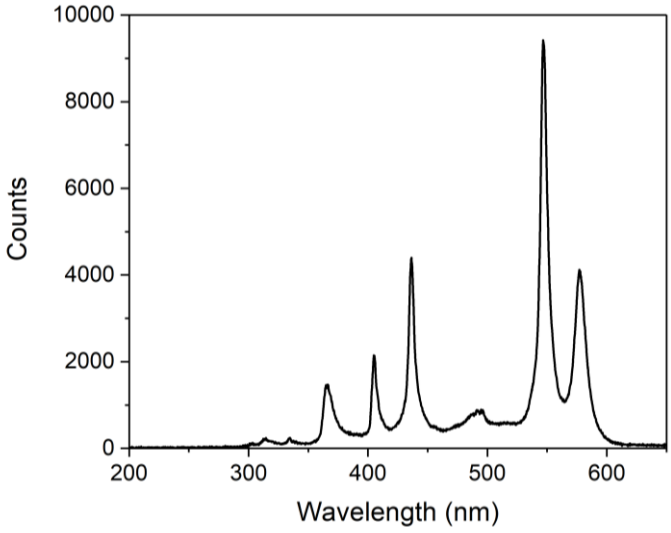

Figure S4. Emission spectrum of the Novacure N2001 light source, measured by a spectrophotometer (HR 2000+, Ocean Optics).

4. Photothermal Heating: On-Off Cycles.

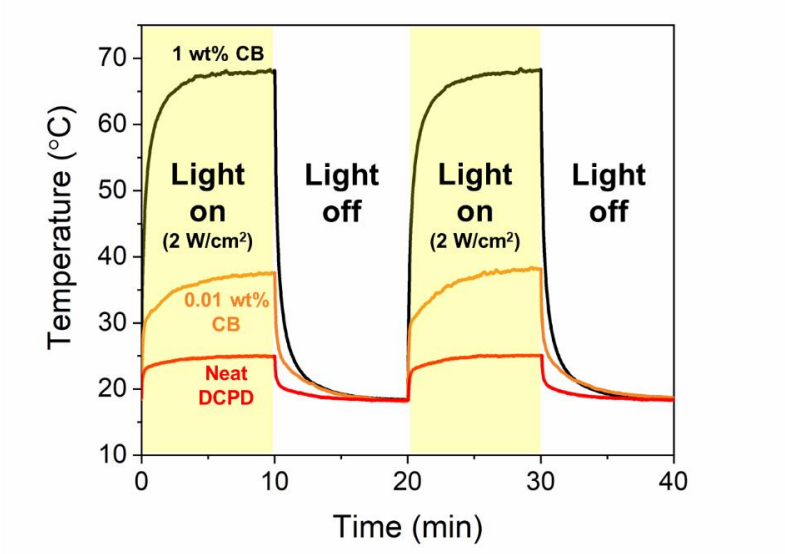

Figure S5. Temperature profiles of CB/DCPD suspensions showing repeatability of temperature rise over multiple cycles. The first cycle is also shown in Figure 2a of the article.

5. Photothermal Initiation of FP: Time to Initiation.

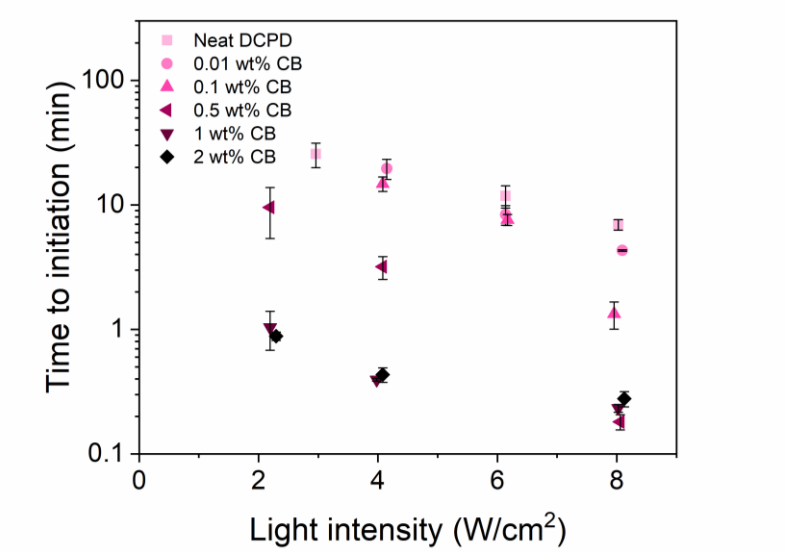

Figure S6. Time to photothermal initiation of FP for CB/DCPD resins with different CB loadings (n = 3 for all data points).

6. Thermal Conductivity Measurements. Nanoparticle/DCPD suspensions were prepared in 30 mL glass vials, and sonicated for 10 min. Immediately after sonication, the thermal conductivity of these suspensions was measured using a TEMPOS thermal properties analyzer (METER Group Inc), which measures thermal conductivity using the transient hot wire method. The instrument was outfitted with a 60 mm KS-3 probe, which was oriented vertically and used in low power mode with 1 min heating time, and 15 min equilibration time between measurements. Precautions were taken to isolate the sample from vibrations and thermal fluctuations during measurement. For each nanoparticle loading, three samples were prepared, and three measurements were made per sample (Figure S7).

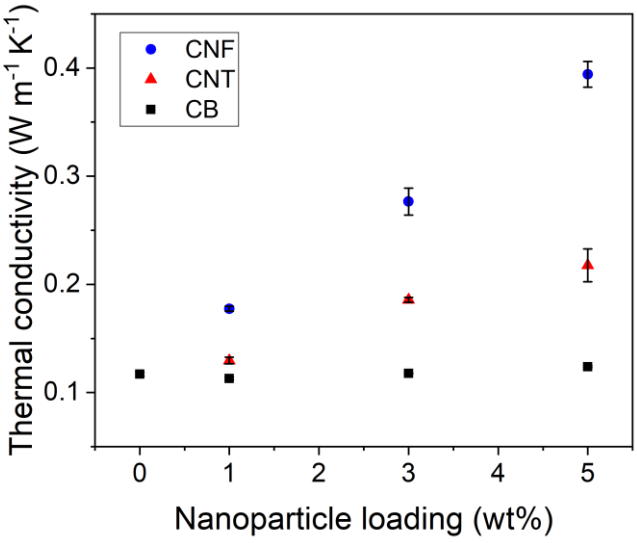

Figure S7. Thermal conductivity measurements of DCPD suspensions with varying amounts of carbon nanoparticles (n = 3 for all data points; error bars represent standard deviation).

7. Viscosity Measurements. Nanoparticle/DCPD suspensions were loaded immediately after sonication into an AR-G2 rheometer (TA Instruments) equipped with 25 mm diameter aluminum parallel plates covered with adhesive backed sandpaper (600 grit, McMaster Carr). Viscosity measurements were performed at a steady shear rate of 10 s^{-1} and a temperature of 25 °C. The viscosity was recorded after the measurement had stabilized. Three measurements were performed for each suspension with gaps of 500 μm, 750 μm, and 1000 μm, and the values were averaged (Figure S8).

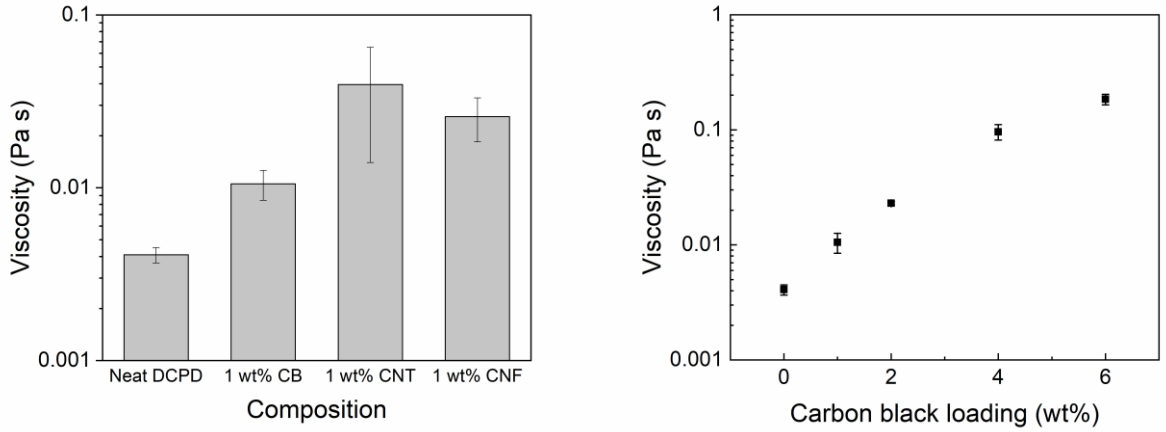

Figure S8. Steady shear viscosity measurements of DCPD suspensions with different nanoparticles (left) and for different loadings of carbon black (right) (n = 3 for all data points; error bars represent standard deviation).

8. Front Velocity Comparison.

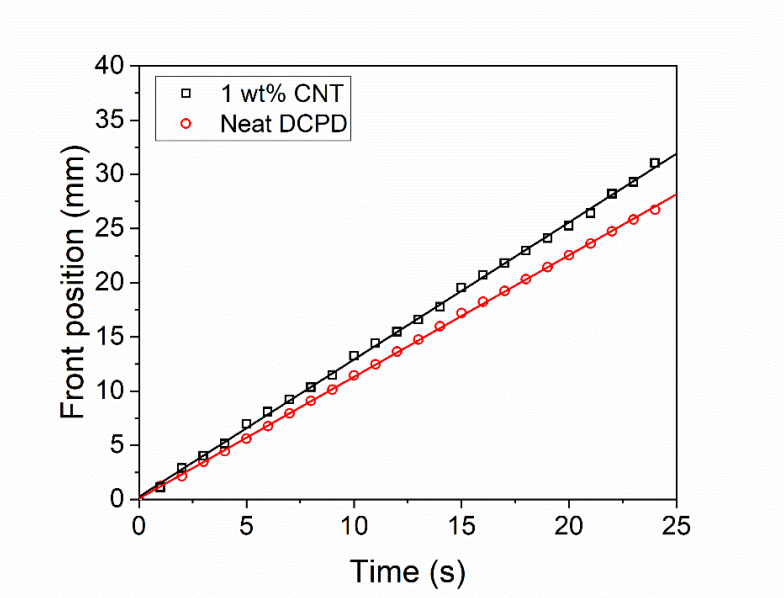

Figure S9. Representative front position vs. time data for front propagation. The slope is equal to the front velocity.

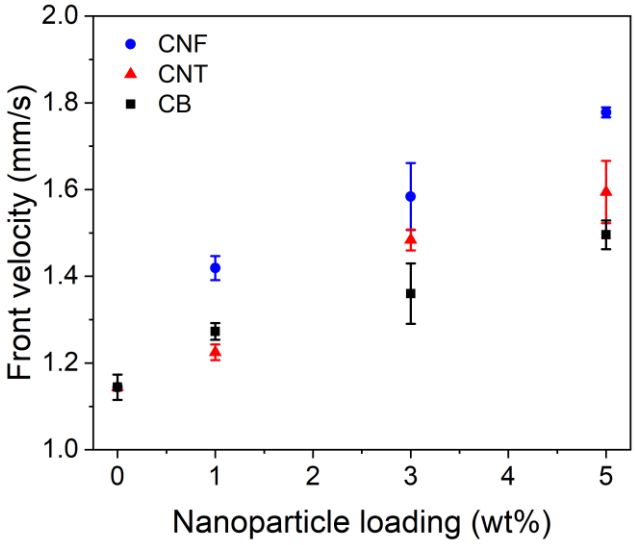

Figure S10. Front velocity as a function of nanoparticle loading (n = 3 for all data points; error bars represent standard deviation).

9. Cure Kinetics. Differential scanning calorimetry (DSC) measurements were performed on freshly prepared nanoparticle/DCPD resin samples (2 – 3 mg each) using a TA Instruments Discovery DSC250. For each composition, three independent scans were performed from –50 to 200 °C at a ramp rate of 7 °C/min. Then, the degree of cure (α) was calculated for each data point in the scan using the following equation:

$$\alpha(T) = \frac{\int_{20\,^\circ\mathrm{C}}^{T} q(T)\frac{dT}{dt}\,dt}{\int_{20\,^\circ\mathrm{C}}^{150\,^\circ\mathrm{C}} q(T)\frac{dT}{dt}\,dt} = \frac{H_r(T)}{H_{r,tot}} \tag{S1}$$

where $q(T)$ is the instantaneous measurement of heat flow and H_r is the heat released during polymerization. Figure S11 shows the average of three scans for each composition.

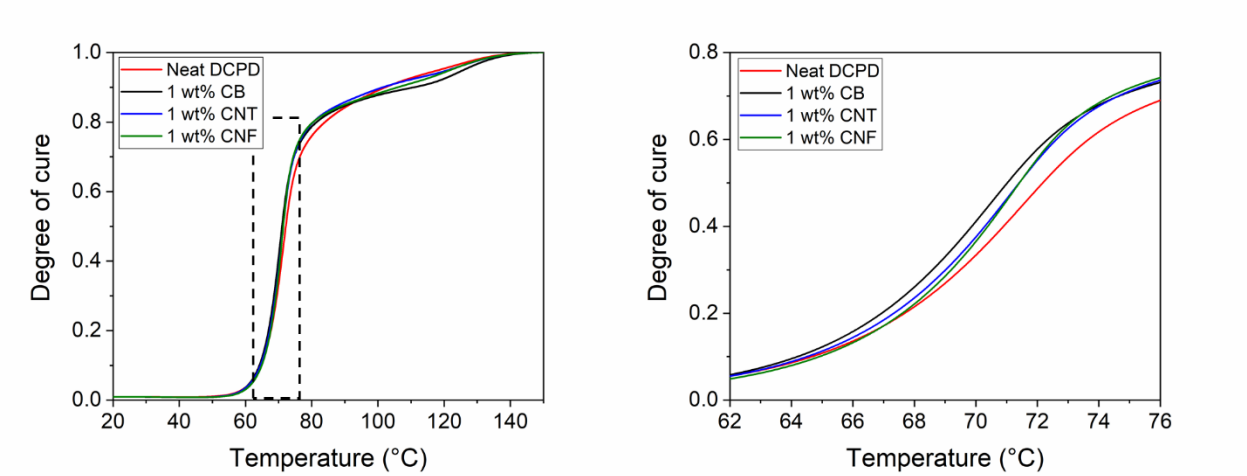

Figure S11. DSC measurements showing slightly accelerated cure kinetics for nanoparticle-containing resins compared to neat DCPD resin. Each curve represents an average of three scans. The right plot is an expanded view of the area indicated by a dashed box in the left plot.

10. Dynamic Mechanical Analysis (DMA). Frontally polymerized samples were machined into rectangular specimens with dimensions of 2 × 2 × 20 mm and measured in 3-point bending using a TA Instruments RSA III. Temperature sweeps were performed between 25 and 200 °C at a nominal strain of 0.3% and a frequency of 1 Hz. The temperature ramp rate was 5 °C/min between 100 and 160 °C and 20 °C/min outside this range. Glass transition temperature (T_g) was extracted from the maximum of tan(δ). Representative DMA curves are shown in Figure S12 and a summary of DMA measurements is given in Table S1.

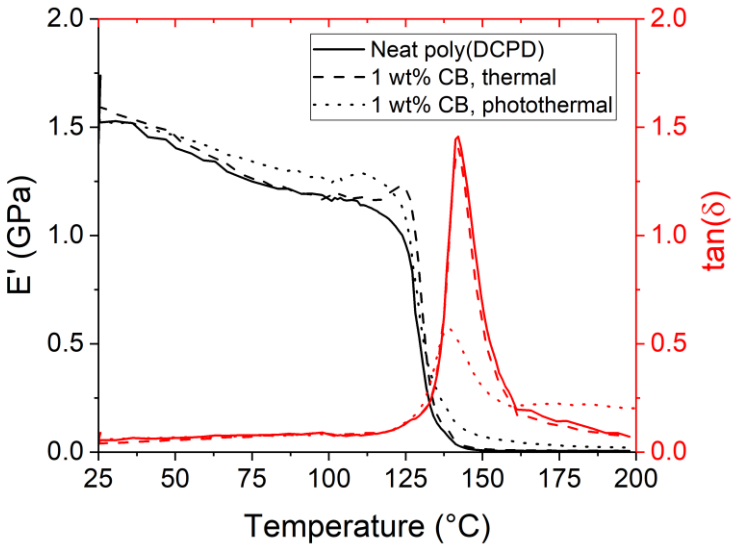

Figure S12. Representative DMA temperature sweep curves showing similar thermomechanical properties for frontally polymerized neat pDCPD and frontally polymerized nanocomposites with 1 wt% CB prepared from both thermal and photothermal initiation.

Table S1. Summary of DMA measurements, where n is the number of specimens tested.

Sample type	FP initiation	n	E′ (GPa) at 25 °C	T_g (°C)
Neat pDCPD	Thermal	6	1.35 ± 0.19	141.6 ± 0.9
1 wt% CB nanocomposite	Thermal	4	1.58 ± 0.03	141.7 ± 0.5
1 wt% CB nanocomposite	Photothermal	4	1.48 ± 0.08	138.6 ± 0.7
1 wt% CNF nanocomposite	Thermal	4	1.50 ± 0.09	140.4 ± 0.5
1 wt% CNF nanocomposite	Photothermal	4	1.35 ± 0.03	141.0 ± 0.9

11. Fracture Toughness Tests. Frontally polymerized samples (neat pDCPD and CB/pDCPD nanocomposites) were machined into single-edge notch bend (SENB) specimens and tested according to ASTM standard D5045. Specimen dimensions were 9 × 19 × 84 mm with a machined notch 7 mm in length. A pre-crack was formed by tapping a fresh razor blade in the notch. Pre-crack length was measured optically using a digital microscope (VHX-5000, Keyence). Mode-I fracture toughness tests were conducted at a crosshead speed of 10 mm/min using an Instron 8841 load frame equipped with a 1 kN load cell and a three-point bending fixture set to a 76 mm span. The critical stress intensity factor, K_{IC}, was calculated according to the referred standard. Results are shown in Figure S13. Some specimens failed in a brittle manner while others failed in a ductile manner, with slow crack propagation. Within each failure category, the differences between specimens with different amounts of CB were not statistically significant. Representative fracture surfaces are shown in Figure S14.

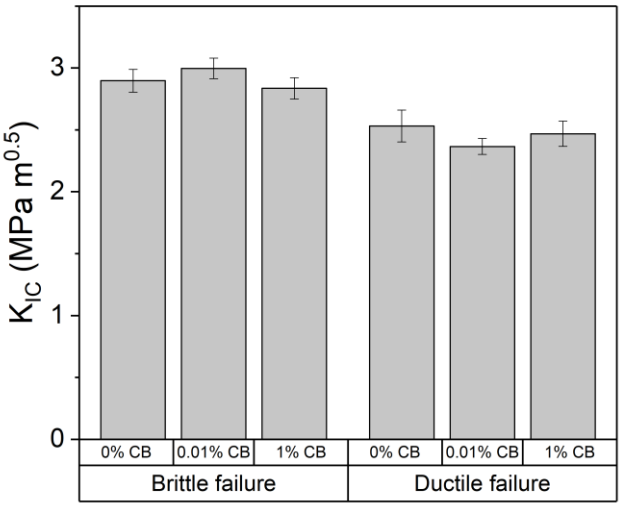

Figure S13. Plane strain critical stress intensity factor (K_{IC}) for frontally polymerized specimens with varying amounts of carbon black.

12. Scanning electron microscopy (SEM). Scanning electron micrographs were taken using an environmental SEM (Quanta FEG 450, FEI Company) operating at 5 kV. The polymer and nanocomposite samples in Figure S14 were sputter coated with a thin layer (ca. 7 nm) of gold-palladium prior to imaging. The nanoparticle samples in Figure 1b of the article were prepared for imaging by solvent casting from DCPD and were not sputter coated.

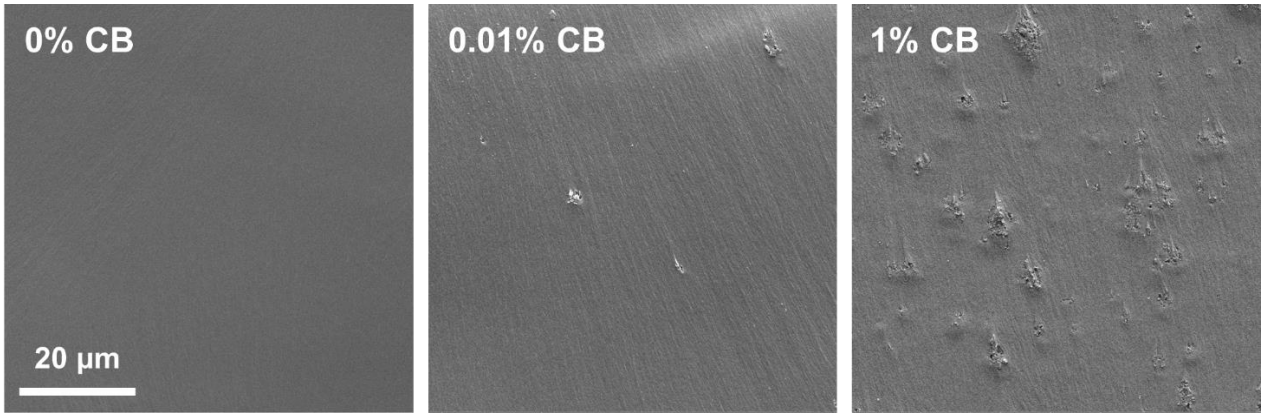

Figure S14. SEM micrographs of fracture surfaces of frontally polymerized specimens with varying amounts of carbon black. Crack propagation is in the vertical direction.